evaluation results in a large figure of misfit mostly due to a large figure of deviation stemming from the elongation in the **b** direction. However, the Dirichlet domains support the relation: the rhombi parallel to **b** are changed to hexagons as a consequence of the elongation in the **b** direction, otherwise there are only small changes.

(vi) The last example refers to the relations among the basic arrangements '*cF*', '*cI*', '*hE*', the cubic *I* lattice may be regarded as being between hexagonal close packing and cubic close packing (see Fig. 6). The quantitative evaluation shows that the relation between '*hE*' and '*cI*' is stronger than between '*cF*' and '*cI*'.

References

BÄRNIGHAUSEN, H. (1975). *Acta Cryst.* A**31**, S3.

BRUNNER, G. O. & SCHWARZENBACH, D. (1971). *Z. Kristallogr.* **133**, 127-133.

DELAUNAY, B. (1933). *Z. Kristallogr.* **84**, 109-149.

EWALD, P. P. & HERMANN, C. (1931). *Strukturbericht* 1913-1928, p. 10.

FISCHER, W., BURZLAFF, H., HELLNER, E. E. & DONNAY, J. D. H. (1973). *Space Group and Lattice Complexes. Natl Bur. Stand. (US) Monogr.* No. 134.

HELLNER, E. E. (1966). *Acta Cryst.* **21**, A252.

HERMANN, C., LOHRMANN, O. & PHILIPP, H. (1937). *Strukturbericht* 1928-1932, p. 5.

LAVES, F. (1930). *Z. Kristallogr.* **73**, 202-265, 275-324.

LIMA-DE-FARIA, J., HELLNER, E., LIEBAU, F., MAKOVICKY, E. & PARTHÉ, E. (1990). *Acta Cryst.* A**46**, 1-11.

MEGAW, H. (1973). *Crystal Structures: a Working Approach.* Philadelphia: W. B. Saunders.

PARTHÉ, E. & GELATO, L. M. (1984). *Acta Cryst.* A**40**, 169-183.

PARTHÉ, E. & GELATO, L. M. (1985). *Acta Cryst.* A**41**, 142-151.

WELLS, A. F. (1954). *Acta Cryst.* **7**, 535-544, 545-554, 842-848, 849-853.

WELLS, A. F. (1955). *Acta Cryst.* **8**, 32-36.

WELLS, A. F. (1956). *Acta Cryst.* **9**, 23-28.

WELLS, A. F. (1975). *Structural Inorganic Chemistry*, 4th ed., p. 329. Oxford: Clarendon Press.

Acta Cryst. (1992). A**48**, 490-494

Observed Rocking-Curve Fine Structure on the *Aufhellung* Side of Renninger-Scan Peaks

BY N. G. ALEXANDROPOULOS

University of Ioannina, GR-45110 Ioannina, Greece and Polytechnic University, Brooklyn, NY 11201, USA

H. J. JURETSCHKE

Polytechnic University, Brooklyn, NY 11201, USA

AND K. T. KOTSIS

University of Ioannina, GR-45110 Ioannina, Greece

(*Received* 11 *July* 1991; *accepted* 7 *January* 1992)

Abstract

Rocking curves of the Si(222) reflection have been measured with σ-polarized incident radiation in the *Aufhellung* region of a Renninger scan near an *n*-beam interaction point. Even with an angular resolution $\Delta\theta = \pm 8''$, much larger than the intrinsic width of this weak reflection, these curves show a structure with two or more peaks, deviating markedly from that of the standard shape of a (convoluted) weak reflection. Details of the structure vary with the azimuthal angular distance from the interaction point, with the reciprocal-lattice vectors involved in the interaction, and with wavelength. Several typical examples of rocking curves obtained under different experimental conditions are presented and the probable origin and consequences of this structure are discussed.

Introduction

In the reflecting plane of a two-beam reflection, the intensity is governed by the deviation from the Bragg angle $\Delta\theta$ and by the setting of the azimuthal angle φ. Rocking curves are obtained by varying $\Delta\theta$ at constant φ and are usually independent of φ, for φ far enough from the *n*-beam interaction point. On the other hand, a typical Renninger scan (Renninger, 1937) records the intensity variation of this reflection, integrated over $\Delta\theta$, as a function of azimuthal angle φ. Such variations occur in the immediate neighbourhood of multiple interaction points, often giving rise to the well known asymmetry which can be used for phase determination (Chang, 1987). The conventional interpretation of the Renninger-scan data assumes that the integration over $\Delta\theta$ is over a standard two-beam line shape. So far, however, experimental

0108-7673/92/040490-05$06.00

verification of this assumption has been lacking. This report presents a study of such line shapes.

Multiple diffraction occurs whenever two or more reciprocal-lattice points lie simultaneously very close to the Ewald sphere. Fig. 1(*a*) shows schematically a typical three-beam interaction. **H** is the primary reciprocal-lattice vector and **L** and **L**′ characterize the coupling reflections at the interaction point $\varphi = 0$. The wave vector **k** receives intensity from the direct reflection of $\mathbf{k}_0$ by **H** and from the indirect reflection of $\mathbf{k}_0'$ ($=\mathbf{k}_0+\mathbf{L}$) by **L**′. Fig. 1(*b*) shows the case for $\varphi \neq 0$, when $h'k'l'$ moves off the Ewald sphere; the two contributions may have different intensities as well as slightly different directions.

Our experiments on Si(222) clearly indicate one peak in the rocking curve whose location in θ is relatively independent of φ and another peak which separates more and more from the first one as φ increases, while also getting smaller in height. Fig. 2 demonstrates the appearance of both peaks, when φ is on the *Aufhellung* side of $\varphi = 0$, where the two contributions to the two-beam reflection presumably contribute by destructive interference, giving a very small net signal. No such effects have been observed on the other (*Umweganregung*) side (Alexandropoulos, Juretschke, McWhan & Kotsis, 1991), where the interference is presumably constructive. Additional much smaller peaks have been seen on the tails of the rocking curves. The various details of our study are presented below. The study demonstrates that the shape of the rocking curves cannot be taken for granted in some regions of the Renninger scan and therefore that interpreting such scans in these regions may require some caution.

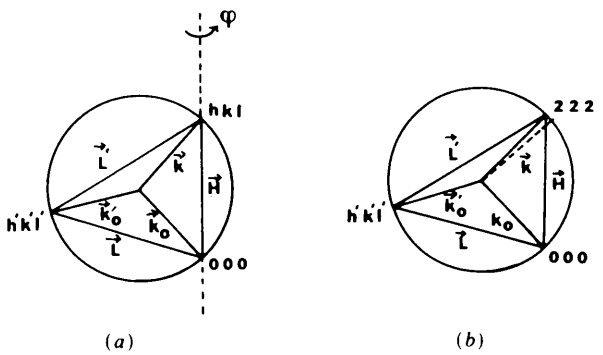

Fig. 1. (*a*) Schematic representation of a three-beam interaction **OHL**. (*b*) Rotating the crystal azimuthally off the three-beam Renninger peak causes a splitting of the **OH** diffracted beam.

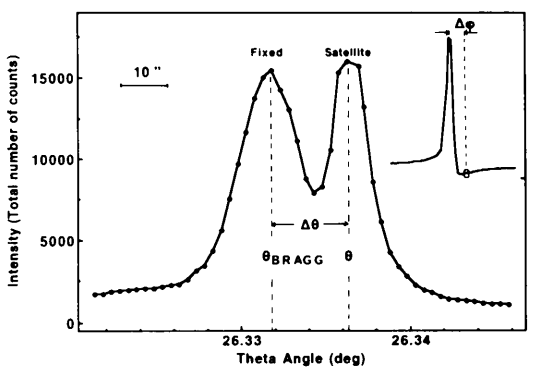

Fig. 2. Typical double-beam structure of the rocking curve of 222 Si, $\lambda = 1.391$ Å at $\Delta\varphi = 126''$ from the four-beam Renninger scan peak (222), (531) and ($1\bar{1}\bar{3}$).

Experiment

This investigation required the resolution, polarization and high intensity only available at synchrotron facilities. We made use of the AT&T Bell Labs facilities of beam line 16C at NSLS BNL (Gmür & White-DePace, 1986). Data were taken at wavelengths 1.277, 1.299, 1.391, 1.497 and 1.540 Å, often for both polarizations, although only σ-polarized data are presented here.

The setup is shown in Fig. 3. The beam was processed through a constant-offset double flat Si(111) crystal monochromator (DCM) (Hastings, Kincaid & Eisenberger, 1978) and a slit system (*S*), to enter a biaxial diffractometer (BD) composed of a two-circle Huber goniometer (TCG), a one-circle goniometer (OCG), a goniometer head (GH) and a base. The ionization chamber (*I*) and the Kapton foil scintillation detector (MD) monitor the incident intensity. With two stepper motors of $\Delta\theta = 0.0005°$, the TCG provides the θ-2θ motion, while the OCG provides the azimuthal rotation in steps of $\Delta\varphi = 0.005°$. The two Huber goniometers are mounted with their axes perpendicular to each other. The goniometer head is positioned with its axis parallel to the OCG axis and the Si(111) sample on it is on a 'stress-free' mount. The TCG is mounted on the flat metallic base which pivots around a horizontal axis permitting the TCG axis to be horizontal or vertical, for the two polarizations (π and σ, respectively).

The adjustments consist of bringing the [111] direction of the crystal onto the rotation axis of the OCG and calibrating the θ-2θ and φ scales for correct reading of the Bragg and Renninger peak angles. Wavelength determination used the perfect Si sample as analyser to measure the Bragg-angle differences for at least two reflections, *e.g.* 333 and 444. The transition from the nominal to the precise values of θ and φ employed the silicon lattice parameter $a = 5.4307$ Å and the appropriate wavelength. To prevent harmonics, the double-crystal monochromator has been detuned for the primary wavelength and a high-energy-resolution pulse-height discrimination has been employed.

Data collection was made in constant monitor counts, accumulating at least 5×10^5 counts at each step in a time not exceeding 2 s.

The system's stability and reproducibility were estimated at two steps by repeating measurements of the rocking curve at the same nominal φ position from a Renninger-scan peak. The insert in Fig. 3 shows the crystallographic orientation and cut of the Si sample.

Results

Fig. 4 shows a typical Renninger scan and its indexing over a large part of the basic 30° range of φ. The typical angular distance between prominent interactions is about 1° and in-between is a flat and φ-insensitive intensity typical of the pure two-beam reflection. The details of location and intensity of the structure vary with wavelength.

Fig. 5 shows the rocking curve of the forbidden 222 reflection, at a distance of about $\varphi = 300''$ from the nearest interaction point. It has a full width at half-maximum of about 15″. Since the theoretical intrinsic width of the 222 reflection is about 0.12″, a value confirmed in recent experimental work (Entin & Smirnova, 1989), the observed width must be entirely due to the angular broadening of the incident beam. As a consequence, we cannot expect to resolve any fine structure of the rocking curve in the many-beam neighbourhood due to intrinsic dynamical effects, since these are usually much smaller than the broadening introduced by the incident beam.

Fig. 6 indicates the changes occurring as the rocking curve is probed nearer to the three-beam interaction point, the (222), (11$\bar{3}$) peak. The square in the Renninger-scan inset locates the azimuthal angle, $\Delta\varphi = -54''$. The solid line now shows two peaks, one at the expected Bragg angle for the 222 reflection ($\theta_B = 24.488°$) and closely matching the dotted curve, a repeat of Fig. 5 (scaled in magnitude), and another peak at $\Delta\theta = -8''$. As the displacement from the interaction point increases, this second peak moves further away and decreases in magnitude.

A similar effect is observed in the *Aufhellung* region near a four-beam point. Fig. 7 gives the rocking curves at three different $\Delta\varphi$ near the interaction (222), (531) and (1$\bar{1}\bar{3}$). Again there is a relatively fixed peak and a peak that is moving away, this time towards higher θ angles, and of rapidly decreasing magnitude.

The relation between $\Delta\theta$ of the satellite peak and $\Delta\varphi$ is illustrated in Fig. 8 for three three-beam interactions and three four-beam interactions, with one four-beam case measured at two wavelengths. In all cases, the relation is close to linear, although the curve does not necessarily intersect the origin.

Discussion

Complicated rocking-curve structures in the neighbourhood of multiple interaction points are covered by dynamical theory (Kon, 1988; Juretschke, 1990), but their angular range is usually of the same order as that of the intrinsic line width of the underlying two-beam reflection. Here, however, as already pointed out, such effects can be expected to be averaged out in the presence of the angular spread of the incident beam. In addition, dynamical effects are expected to be coherent, while the survival of different peaks at such large angles points to an incoherent superposition of different effects. It is therefore most likely that they arise from interactions associated with the angular spread of the incident beam, which is of the same order of magnitude as the observed angular shifts.

Such a spread, in fact, illuminates not only the two-beam **O–H** region of the Ewald sphere, but, for example, in the neighbourhood of the **O**, **H**, **L** three-beam point it will also continue to illuminate the two-beam **O–L** region for some distance $\Delta\varphi$ away from the interaction point, as was suggested geometrically in Fig. 1. In this case, we will observe the confluence of three-beam interactions in the two

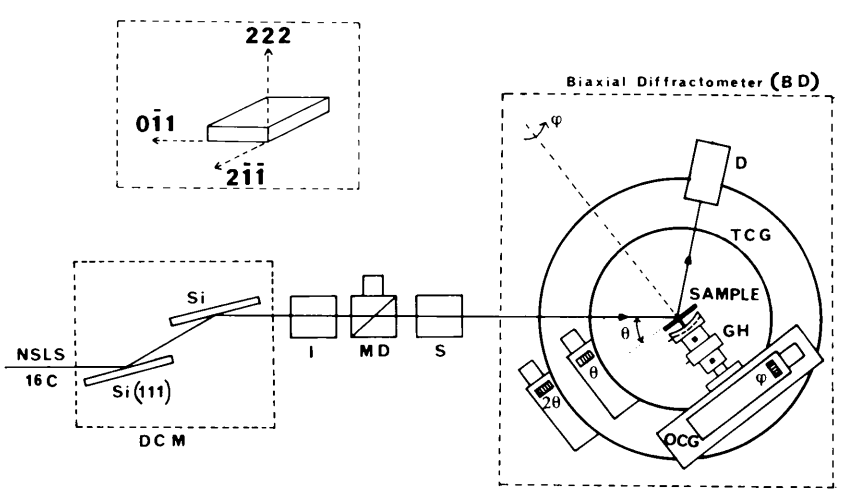

Fig. 3. Diagram of the equipment.

two-beam interactions as the three-beam point is approached. As a first test of this hypothesis, we have calculated the geometrical rate of separation $\Delta\theta$ in the **O–H** plane of the **H** reflections from the two two-beam circles *OH* and *OL* of the intersecting Ewald spheres, as the **O–H** plane moves away from the geometrical three-beam point. The evaluation has been carried out for all the cases given in Fig. 8. As shown in Table 1, this rate of separation $\Delta\theta/\Delta\varphi$ is of order unity and can be of either sign. Comparison with Fig. 8 indicates that the signs agree fully for all three-beam cases. In the three four-beam cases (each really a superposition of two three-beam cases), the signs agree with one of the three-beam contributions, but not with the other. In addition, the trend towards smaller values with increasing wavelength, noted in the points for (222) (531) and $(1\bar{1}\bar{3})$ in Fig. 8, is in agreement with the calculations. However, all of the magnitudes of the observed shifts are smaller than those of Table 1.

A number of considerations must, however, be kept in mind. Most importantly, even though the input beam was σ polarized in all cases, near the interaction point the proper modes in the crystal have more complicated polarization (Juretschke, 1990), so that

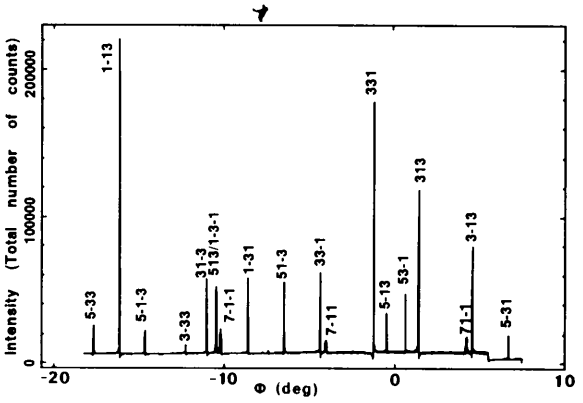

Fig. 4. Renninger-scan chart over much of the basic angular range of 30°, obtained in steps of $\Delta\varphi = 0.005°$ using a σ-polarized incident beam at $\lambda = 1.497$ Å.

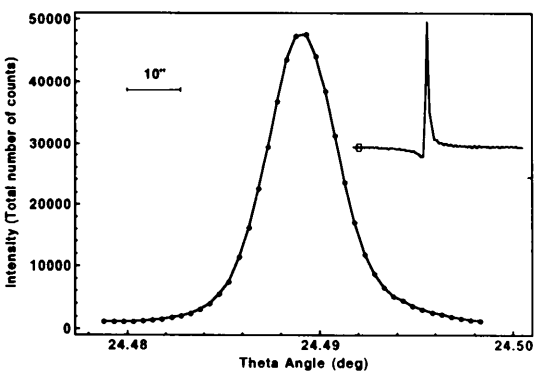

Fig. 5. Rocking curve of the Si 222 reflection, $\lambda = 1.299$ Å, far from the nearest interaction peak $(222)/(11\bar{3})$, as shown in the inset.

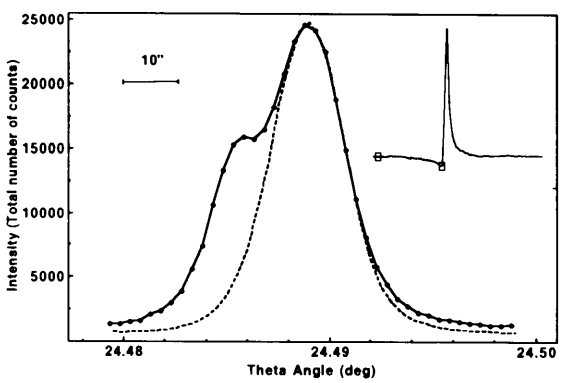

Fig. 6. Rocking curve of the Si 222 reflection at $\Delta\varphi = -54''$ from the $(222)/(11\bar{3})$ peak. $\theta_B = 24.488°$ and $\Delta\theta = -8''$. The inset shows the location of $\Delta\varphi$ relative to the overall structure of the Renninger scan. The dashed curve is that of Fig. 5, with adjusted amplitude.

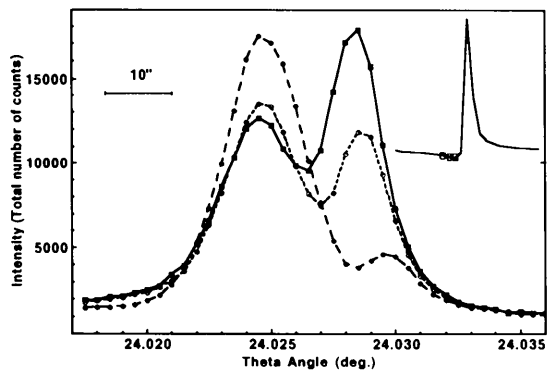

Fig. 7. Three rocking curves of (222), (531) and $(1\bar{1}\bar{3})$ at different distances from the interaction point. —■—: $\Delta\varphi = -45''$; ---○---: $\Delta\varphi = -63''$; ---●---: $\Delta\varphi = -81''$. Their locations are shown in the inset. $\lambda = 1.277$ Å.

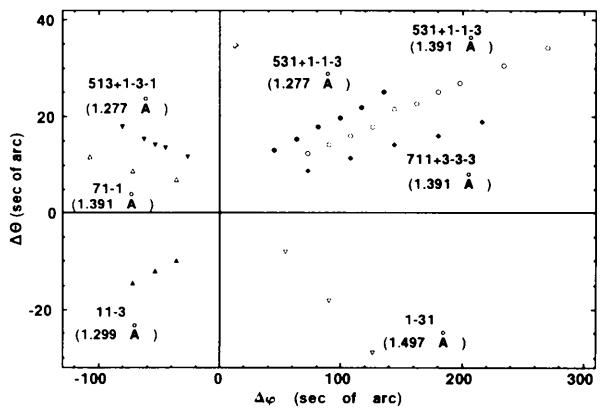

Fig. 8. Shifts $\Delta\theta$ of the satellite peak as a function of $\Delta\varphi$ near several three- and four-beam interactions at a number of wavelengths.

Table 1. *Calculated ratio $\Delta\theta/\Delta\varphi$ of the geometrical shift in reflection angle $\Delta\theta$ along* **H** *due to the two-beam interaction* **O–L** *near the* **OHL** *three-beam point.*

$\Delta\varphi$ is the azimuthal angular deviation from this point along the two-beam reflection **O–H** (see Fig. 1). Each of the four-beam cases is a superposition of two three-beam cases.

λ(Å)	H/L	$\Delta\theta/\Delta\varphi$
Three-beam cases		
1.299	(222)/(11$\bar{3}$)	2.05
1.391	(222)/(71$\bar{1}$)	−1.82
1.497	(222)/(1$\bar{3}$1)	−1.53
Four-beam cases		
1.277	(222)/(513) (222)/(1$\bar{3}$1)	0.425 −0.662
1.277	(222)/(531) (222)/(11$\bar{3}$)	−0.425 0.662
1.391	(222)/(531) (222)/(11$\bar{3}$)	−0.363 0.494
1.391	(222)/(711) (222)/(2$\bar{3}\bar{3}$)	−0.464 0.327

more than one of the modes inside the crystal is being excited. Since each of these modes has its own dynamical three-beam point, usually shifted from the geometrical one, the measured $\Delta\varphi$ represents some sort of complicated average. In fact, theory for (222) (11$\bar{3}$) based on a single three-beam interaction gives a theoretical $\Delta\varphi$ smaller by about 20″ than the one recorded, such as in the inset in Fig. 6. In addition, because of the dynamical shifts of the $O-L$ contribution, in the (222) (11$\bar{3}$) case certainly of the order of 1″ the straight-line relation will break down close to the three-beam point. Finally, the magnitude and spread of each of the two observed peaks is expected to be a superposition from all six sheets of the dispersion surface, excited over the full angular range of the incident beam. Hence both the relative and the absolute location of all peaks is subject to considerable uncertainty with respect to any simple theoretical model based on a single mode excited at a single incident angle. In particular, such a model is insufficient to understand why, if our basic explanation is correct, only one of the two satellite peaks expected in four-beam cases is observed. The same insufficiency also applies to the case for three-beam interactions where the possible satellite peaks are very weak (Fig. 9, in fact, shows two such peaks). For a fully quantitative comparison, one would obviously have to know the shape of the incident beam as a function of both angles θ and φ.

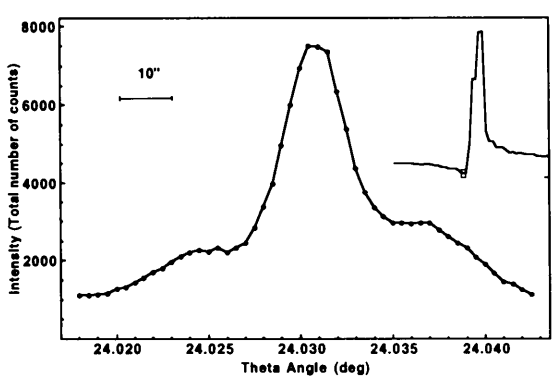

Fig. 9. Weak rocking-curve structure near (222)/(331). $\Delta\varphi = -126''$.

We conclude that the observed complicated rocking-curve structure near the dip in the Renninger scans is most probably due to the angular spread of the incident beam, small as it is by normal standards in X-ray experiments. This implies that all detailed interpretations of very weak intensities observed in multiple-beam interactions are subject to the same uncertainty. For example, Fig. 4 suggests that the true intensity at the Renninger-scan minimum may be reduced through such an effect by at least a factor of order 2. This is probably one of the reasons why observed dips are never as sharp and as deep as simple single-excitation theory predicts. Such prediction can make full quantitative contact with experiment only if the incident-beam angle is defined much more sharply, especially along θ, and if the diffracted output is also analysed as a function of polarization.

References

ALEXANDROPOULOS, N. G., JURETSCHKE, H. J., MCWHAN, D. & KOTSIS, K. T. (1991). *Nucl. Instrum. Methods*, **A308**, 282-284.
CHANG, S. L. (1987). *Crystallogr. Rev.* **1**, 87-189.
ENTIN, I. R. & SMIRNOVA, I. A. (1989). *Acta Cryst.* **A45**, 577-580.
GMÜR, N. F. & WHITE-DEPACE, S. M. (1986). NSLS User Manual, Brookhaven National Laboratory, Upton, NY, USA.
HASTINGS, J. B., KINCAID, B. M. & EISENBERGER, P. (1978). *Nucl. Instrum. Methods*, **152**, 167-171.
JURETSCHKE, H. J. (1990). *Acta Cryst.* **A46**, C416.
KON, V. G. (1988). *Sov. Phys. Crystallogr.* **33**, 333-336.
RENNINGER, M. (1937). *Z. Phys.* **106**, 141-176.